DATA AGGREGATION BASED HYBRID DEEP LEARNING TECHNIQUE FOR IDENTIFYING THE UNCERTAINTIES AND ACCURATE OBJECT DETECTION

Sreehari Patibandla

Research Scholar, Department of Computer Science & Engineering, Annamalai University, Chidambaram Tamil Nadu,608001, India.
sreehari.44@gmail.com

Dr. Maruthavanan Archana

Assistant Professor, Department of Information Technology, Annamalai University, Chidambaram Tamil Nadu, 608001, India.
archana.aucse@gmail.com,

Dr. Rama Chaithanya Tanguturi

Professor, Department of Computer Science & Engineering, PACE Institute of Technology and Sciences, Ongole, Andhra Pradesh, 523272, India.
trchaitanya@gmail.com

Abstract:
The deep learning concept for performing object detection plans to minimize the labeling cost by identifying the samples which increase the detection into the unlabeled pool. According to the object detection than the classification process as the designing and selection of procedure is very essential. The related works have been implemented the aggregation data process of several outputs and batch box process for improving the performance evaluation. The mean Average Precision (mAP) is the main performance metric for identifying the accuracy of the object detection. The class imbalance problem has been solved using the background class in every group of sample images. The loss related weight algorithm for training group is proposed in this paper utilizing the batch boxes, aggregating data and also the mAP enhancements are addressed to solve the class imbalance problem. Additionally, a sampling process is used for identifying the uncertainty and enhancing the object detection process. The performance results illustrate that the proposed framework generates good performance than the relevant technique and it will be used for real-time applications in an efficient manner.

Keywords: **Object detection, cross entropy, best gradient value, Batch loss, mAP, deep learning.**

1. Introduction

The object detection is a complex task in computer vision field that several techniques have been implemented to achieve the object detection more accurately. The objects in satellite images are very different than the natural objects that achieves very difficult in accurate object detection [1]. The current works have the rotation related detectors for detecting the arbitrary related objects in satellite images, these kinds of detectors are initially completed during the preprocessing with a huge number of prior boxes for aligning the ground truth of the objects [2]. The samples have been segregated as the positive and negative samples due to complete the regression of the bounding box with the Intersection over Union (IoU) concept [3]. The entire procedure is demonstrated as the label assignment, according to the real fact as the objects n, the satellite images have huge number of variations like shape, orientation, bounding boxes, and shape which requires forcing the matching of objects. Hence, the dense related training sample identification technique is demonstrated as the dense assignment of labels.

The dense assignment of labels generates complex issues for object detection in satellite images. Initially, several predefined bounding boxes have the backgrounds like unbalancing while training specifically the single stage detectors. Additionally, the dense prediction produces the inconsistency problem within the regression and classification while object detection. Particularly, the dense based bounding boxes have to be included in several positive samples that detect the similar objects [4]. Moreover, the huge classification scores could not assure the

improved localization results. Hence, the false duplication detections could occur after the object classification process. Additionally, the object detection through dense in satellite images suffers according to the assignment of dense label and missed directions. The detection from the output box has the lowest localization accuracy minimizes the highest accuracy which will produce the missed directions. The dense positive samples have the huge overlapping directions. Hence, the particular classification scores are not efficient in demonstrating the accuracy of localization that leads to the minimized performance of object detection.

2.   Related works

The object detection techniques are classified into the group of single-stage and multi-stage detectors for achieving quality-based object detection. The inference speed of the detector is very fast and the accuracy for detecting the object is smaller. For achieving good performance of detection, the dense-based detection has the bounding boxes to produce the enhanced spatial-based ground truth of objects where the highest IoU based samples having the positive samples of training [5]. The regression related offset technique [6] maintains the metrics of search space and obtains the convergence. Moreover, a huge amount of predefined bounding boxes is needed for producing better spatial alignment through the improved semantic knowledge, it will cause the performance degradation. For solving these kinds of issues, a group of sampling techniques have been implemented to identify the unbalance within the training samples. The focal loss minimizes the sample weights for avoiding the huge number of negative samples. The harmonizing technique with gradient value has been implemented to maintain the balance from the dissimilar samples.

The object detection in satellite images has been enhanced through the group of application values. The angle-based prediction technique [6] involves the detectors for locating the objects in satellite images. Even though these techniques have the enhanced performances, the huge variation in shape, orientation, and scaling of objects in the satellite images have been identified and hence couldn't increase the performance of the detection. Several rotation detectors [7] have been implemented for improving the detection accuracy. The attention related features with local contexts are used for detecting the objects in dissimilar scales. A unified feature related technique is used to produce the context data in different scales for enhanced object detection. The regression-based technique called as CFC-Net [8] is used for producing the feasible classification process. A feature-fusion related framework [9] is used to solve the issue of multi scale feature strategy. The semantic representations are combined with the shallow layers to identify the feature maps of layers through low-level data which utilizes to perform the object detection in multiple scales.

The oriented object representation [10] is a specific issue of object detection in satellite images that has been implemented in lot of similar works. The representation of related rectangle is the huge bounding related issues which produces the problem of convergence. The fine-grained angle classification technique [11] is used to reduce the out of bounds angles. The enhanced regression optimization with bounding box concept has been implemented for unifying the boundary conditions for improved optimization. The inconsistency within the loss and the localization accuracy through the oriented rectangle related boundary issues that have been eliminated through the regression optimization in consistent way.

Several label assignment techniques [12] have been implemented for increasing the object detection in satellite images. The generic object detection concept [13] is one of the features of label assignment technique that the negative and positive values are used to maintain the threshold value of pre-defined IoU values. The rotation-based satellite object detection technique [14] has been included the label assignment techniques. The inconsistency of localization capability has been improved through the boundary box regression and rotation-based object detection.

3.   Proposed Framework

The proposed technique is developed with the deep learning concept as every cycle contains the training models, identifying the samples through the dataset. According to the generated error reduction, the most appropriate model is used to demonstrate the image data through the least confidence technique. The deep classifier is generated for computing the entire world's data to the issue of computing the data. The batch determination technique is used to solve the class imbalance problem which has been reduced in some level and the entire process is illustrated in Fig. 1.
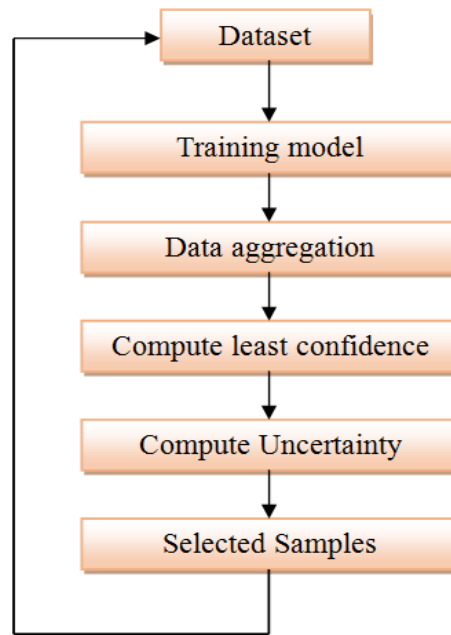
Fig. 1 The overall architecture for the proposed technique

The sample uncertainty is used for computing the error reduction while the least confidence is the main parameter for implementing the uncertainty related technique. The least confidence value is computed for providing the solution for image classification related issue in Eq. (1).

$$\delta_{LC}^{*} = \underset{\alpha}{\mathrm{argmax}}\left(1 - \mathrm{Pr}_{\theta}\left(\hat{\beta}|\alpha\right)\right) \qquad (1)$$

Where $\hat{\beta}$ is the posterior probability for the θ function, the highest probability $\hat{\beta}$ is identified for the predicted class, it is computed in Eq. (2)

$$\delta_{LC}^{*} = \underset{\alpha}{\mathrm{argmax}}\left(1 - \mathrm{Pr}_{\theta}(\beta|\alpha)\right) \qquad (2)$$

While the value of $\mathrm{Pr}_{\theta}(\beta|\alpha)$ is equal to 1, the highest level of accuracy is maintained into the predicted model which has the largest learning value for the particular image. The gradient length is used to compute the discriminative probability in a classical approach. The label is included as the latest gradient for training with higher magnitude, where $\nabla f_{\theta}(\gamma)$ is the objective function through the parameter of θ. The latest gradient $\nabla f_{\theta}(\gamma \cup (\alpha, \beta))$ is generated by including the tuple for training $\langle \alpha, \beta \rangle$ to γ. The gradient length is computed using Eq. (3).

$$\delta_{GL}^{*} = \underset{\alpha}{\mathrm{argmax}} \sum_{i} Pr_{\theta}(\beta_{i}|\alpha) \, ||\nabla f_{\theta}(\gamma \cup \langle \alpha, \beta \rangle)|| \qquad (3)$$

The approximation for minimizing the computational complexity is demonstrated in Eq. (4).

$$\nabla f_{\theta}(\gamma \cup \langle \alpha, \beta \rangle) \approx \nabla f_{\theta}(\langle \alpha, \beta \rangle) \qquad (4)$$

The produced output layer for image classification is computed in Eq. (5).

$$O = (O_{1}, O_{2}, \ldots, \ldots, O_{k}) \qquad (5)$$

The computation of the cross entropy is used for loss function and the Softmax function which is computed in Eq. (6).

$$\sigma(\omega)_i = \frac{e^{\omega_i}}{\sum_{j=1}^{k} e^{\omega_j}} \qquad (6)$$

The mapping function to the output model is computed in Eq. (7) and Eq. (8).

$$f_{EL}(Pr, \beta) = f_{EL}(S(\theta_{out}), \beta) \qquad (7)$$

$$f_{EL}(Pr, \beta) = -\sum_{i=1}^{k} \beta_i \log\left(\frac{e^{\omega_i}}{\sum_{j=1}^{k} e^{\omega_j}}\right) \qquad (8)$$

The highest entropy loss with the output model is computed in Eq. (9).

$$\nabla f_{\theta_{out}}(\gamma) = \frac{\partial}{\partial W t_i} f_{EL}(Pr, \beta) = Pr - \beta \qquad (9)$$

The updated gradient length is computed in Eq. (10).

$$\delta_{GL}^* = \underset{\alpha}{argmax} \sum_{i=1}^{k} ||Pr_i - I(\hat{\beta} = i)|| \qquad (10)$$

The Bet Gradient value is computed in Eq. (11).

$$\delta_{GL}^* = \underset{\alpha}{argmax} \sum_{i=1}^{k} Pr_i = 1 - Pr_\theta(\hat{\beta}|\alpha) \qquad (11)$$

The value of $\hat{\beta}$ is computed in Eq. (12).

$$\hat{\beta} = \underset{\beta}{argmax} \, Pr_\theta(\beta|\alpha) \qquad (12)$$

The modified Bet Gradient value is computed in Eq. (13).

$$\delta_{GL}^* = \underset{\alpha}{argmax}(1 - Pr_\theta(\hat{\beta}|\alpha)) \qquad (13)$$

The predicted error reduction technique utilizes to identify the level of generalization error that needs to be minimized. The main aim of the loss function is to reduce the predicted loss and also the computational complexity. The samples with highest loss are used the entropy loss and it is used to discover the sample with highest loss which is computed in Eq. (14).

$$\delta_{EL} = \underset{\alpha}{argmax} \, f_{EL}(Pr_\theta(\beta_i|\alpha), \beta_i) \qquad (14)$$

The expected label $\hat{\beta}$ has the truth value with highest loss is computed in Eq. (15).

$$\delta_{EL}^* = \underset{\alpha}{argmax} - \log(Pr_\theta(\hat{\beta}|\alpha)) \qquad (15)$$

The predicted model has the error value which performing the image classification whenever the prediction model is obtained the expected result. The consistency aims to find the classifier of the batch of images in every round which has the scores of every image that requires maintaining the single score and the comparison of 2 batches are illustrated in Eq. (16).

$$-\sum Pr_\theta(\hat{\beta}|\alpha_i \in B_1) < -\sum Pr_\theta(\hat{\beta}|\alpha_i \in B_2) \qquad (16)$$

The ranking-based functionality through the classification and regression loss has the correlation of computing the relationship within the losses. The coefficient of rank correlation is the statistical function through the regression and classification. The well-trained model is developed through the dataset with the obtained loss. The computation of the rank correlation of every loss sequence as $\{(\alpha_i, \beta_i)\}_{i=1}^n$ demonstrates the loss sequences, the Kendall correlation R_K is computed in Eq. (17).

$$R_K = (\alpha_i, \beta_i) = \frac{\sum_{i=1}^n \sum_{j=1}^n (\alpha_i - \alpha_j)(\beta_i - \beta_j)}{n^2 - n} \qquad (17)$$

The Spearman coefficient R_S is computed in Eq. (18).

$$R_S = 1 - \frac{6 \sum_{i=1}^n (A_i - B_i)^2}{n^3 - n} \qquad (18)$$

Where A_i and B_i are the rank for β_i and α_i respectively. The correlation coefficient within the two sequences is closed to the value of 1. The highest-ranking correlation with the total loss is appropriately huge, so the total ranking data after completing the classification will minimize the computational complexity. The gradient data of an image has one batch which requires the aggregated score of the optimizer-based classifier model. The batch gradient is the mean batch value, the batch gradient value is computed in Eq. (19).

$$B_G = \frac{1}{m} \sum_{j=0}^k \left\| \sum_{i=1}^m A_{ij} - I(\hat{\beta}_i = j) \right\| \qquad (19)$$

The batch loss data is computed in Eq. (20).

$$L_G = \frac{1}{m} \sum_{i=1}^m - \log\left(A_\theta(\hat{\beta}_i | \alpha_i)\right) \qquad (20)$$

The background class is generated in every batch of images which involves a high-class imbalance. Hence, the elimination of the negative impact while performing the classification process, the background boxes are used while processing the initial state of training with the loss value is randomly evaluated the gradient batch which involves the gradient values of remaining classes. The model has to be trained for reducing the loss of one class and also the remaining classes into the similar time period. The proposed classifier has the gradient and loss values while performing the training procedure in the background loss category. The gradient summary value of the output layer determines the batch related background group. In this initial stage, the gradient loss while training is much higher than the object class that demonstrates an unbalanced stage. According to the initial computation process, the values of weight $wt = (wt_0, \ldots, \ldots, wt_k)$ as the weight based gradient batch value are computed in Eq. (21).

$$WB_G = \frac{1}{m} \sum_{j=0}^k wt_j \left\| \sum_{i=1}^m A_{ij} - I(\hat{\beta}_i = j) \right\| \qquad (21)$$

The weight-based batch loss data is computed in Eq. (22).

$$WL_G = \frac{1}{m} \sum_{i=1}^m - wt_{\hat{\beta}_i} \log\left(A_\theta(\hat{\beta}_i | \alpha_i)\right) \qquad (22)$$

The proposed technique is used to compute the gradient and loss values without disturbing the remaining classes. Initially, the training set is constructed to identify the losses of every boundary boxes. The initial weight of every class is computed from the mean loss of every class, the weight demonstrates the comparative performance of every category in the training set and identify the losses of boundary box that utilizes the predicted values are the ground truth labels. The summation of losses is computed that it could not be modified while including weight of losses, again computed the group of losses of every category to keep the balance within the object classes and background values.

4.Theorems

Algorithm 4.1 – Loss related weight algorithm for training group

Input: Training group Tr, the group of classes Cl
Output: Group of weight wt parameters

 Initialize loss values and weight values
 for every $i \in Tr$ do
  compute the boundary boxes B
 for every $b \in B$ do
  Cl = value of b with ground truth
  ls = classification loss
  $L_1[Cl] = L_1[Cl] +\ ls$
 for every $cl \in Cl$ do
  $wt[cl] = Average\ (L_1[cl])$
 for every $i \in Tr$ do

  compute the boundary boxes B with the respected model

  ls = classification loss with the predicted truth value

$$L_2[Cl] = L_2[Cl] +\ ls$$

 for every $cl \in Cl$ do

  $$Ss_0[cl] = \sum L_2[cl]$$

  $$Ss_1[cl] = \sum (L_2[cl] * wt[cl])$$

  Compute the ratio as $r = \dfrac{\sum(Ss_0)}{\sum(Ss_1)}$

 for every $cl \in Cl$ do

  $$wt[cl] = wt[cl] * r$$

The sampling process is used to compute the information score as the highest value scores are categorized into the samples group. The batch related learning process has the best samples with query values as the uncertainty data has been eliminated for further processing.

Algorithm 4.2 – Sampling process

Input: Labeled group Ls, unlabeled group Us, budget bu, total candidates as n
do
 The samples of Us with the distance value $ds_i = \min \Delta(\alpha_i, \alpha_j)$ in reverse order
 discover the highest n values from the group of candidates
 $Sa = \underset{i \in Cl}{argmax}\ WB_G(\alpha_i)$
 $Sa = Sa \cup bu$
while $|Sa| = bu$

5. Performance analysis

The FLIR dataset [15] has been used for providing the bounding boxes of different categories of objects with 5856 images in the training model through the unlabeled pool which are merged with the validation set. This test has been utilized for analyzing the performance of the proposed technique; the basic baseline functionality is used for training on the random images from the unlabeled pool. The mean uncertainties for predicting the bounding boxes are calculated as the images with the high values which have been selected for the classification process. The testing test has been plotted through the sample images for several techniques for mAP with the dataset. From the initial round of analysis, the mAP is larger than the related techniques; the performance of the several techniques has been analyzed from the dataset with several samples as huge similarity. The balance between the uncertainty and diversity has been analyzed through the sampling process. The training process is

completed with the data augmentation procedure as the input images are flipped into horizontally through the multi-state testing with enabled soft suppression. The proposed technique is compared with the related techniques of RRPN [16], RRD [17], IENet [18], and DRN [19].

The average precision with IoU threshold value is used for measuring the performance evaluation as various scales of the input images are utilized for the experiments. AP_{40} is the average precision with threshold 40%, AP_{80} is the average precision with threshold 80%, AP_{small} is the small-scale average precision, AP_{mid} is the middle scale average precision, AP_{large} is the large-scale average precision value which is illustrated in Fig. 2.
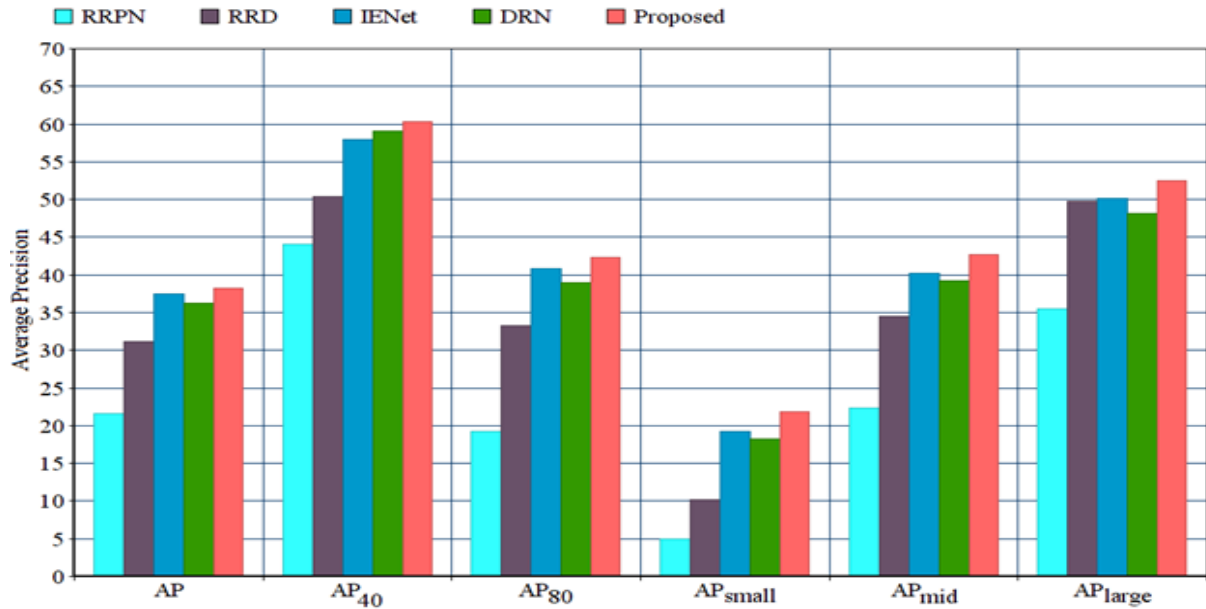

Fig. 2 Average precision

The average recall rate is the important performance metric in performance evaluation as AR_{20} is the average recall with threshold 20%, AR_{90} is the average recall with threshold 90%, AR_{small} is the small-scale average recall, AR_{mid} is the middle scale average recall, AR_{large} is the large-scale average recall in Fig. 3.
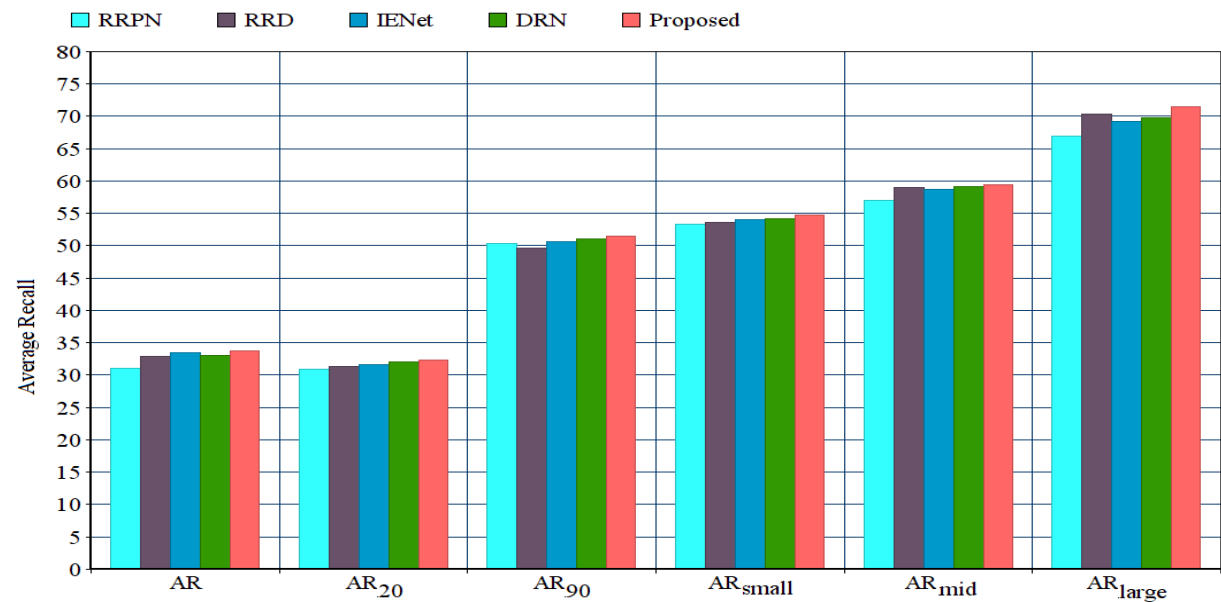

Fig. 3 Average recall

The detection accuracy is evaluated from the efficiency of dissimilar detectors, the time needed to perform the object detection is demonstrated in Fig. 4. The performance result proved that the proposed technique has the minimized amount of time required to complete the process than the relevant methodologies.
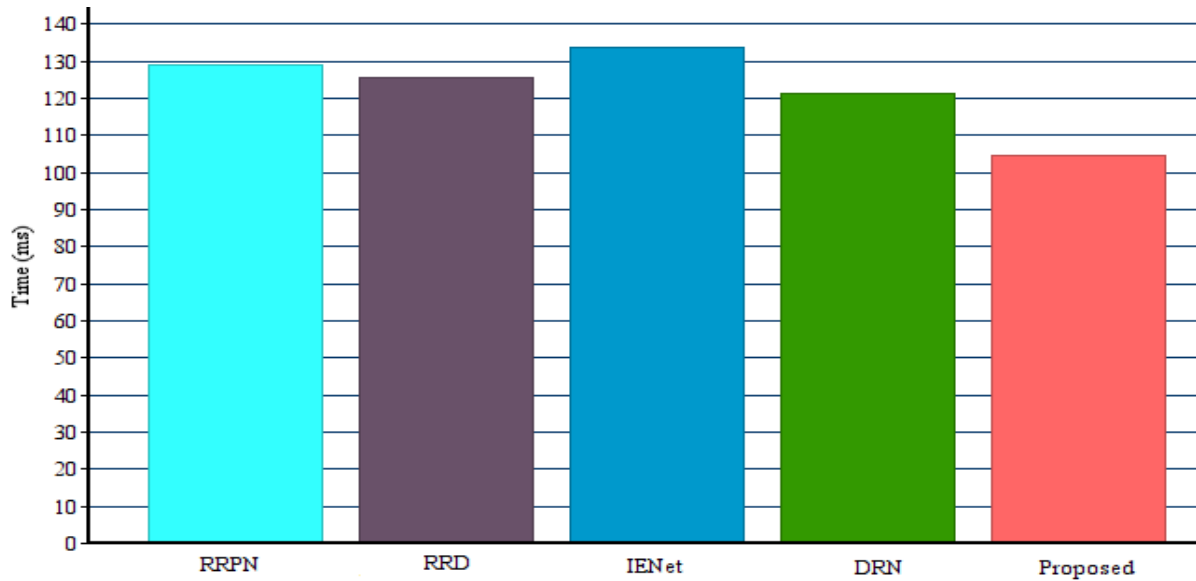

Fig. 4 Time needed for object detection

The overall average precision parameter is used to evaluating the performance of the detection functionality which is illustrated in Fig. 5.
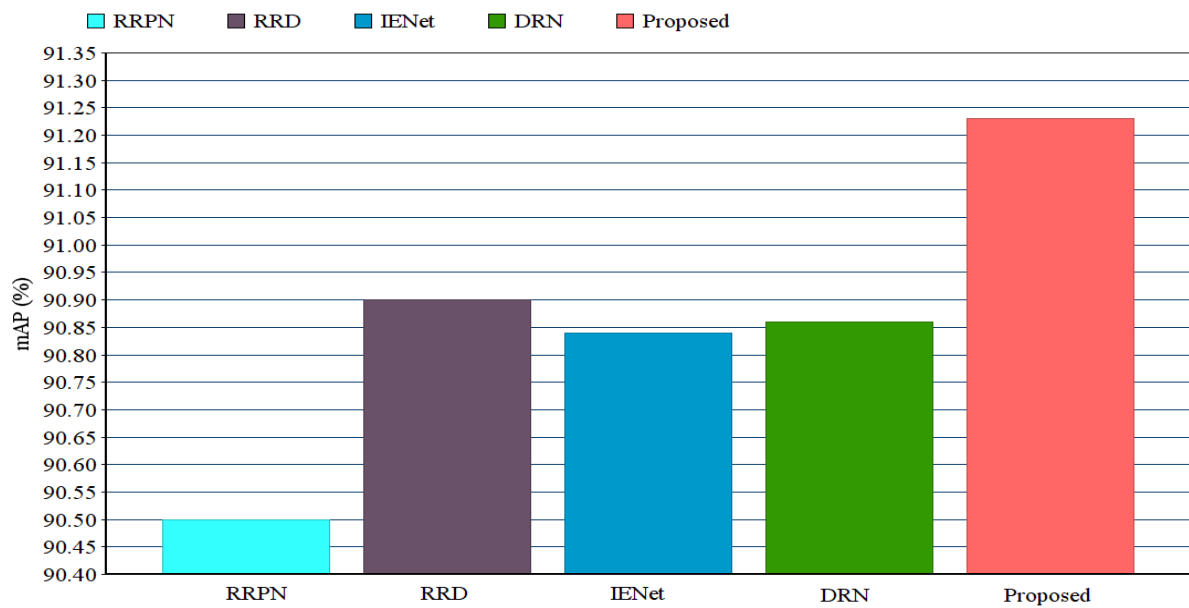

Fig. 5 *mAP*

A detector must demonstrate the interferences of the whole images while the multi-stage detector performs using the cropping the whole feature map and optimizing the back propagation process to obtain the semantics. The proposed technique has been developed to enhance the detection accuracy which is increased in several extra parameters and the average precision for object detection is illustrated in Fig. 6
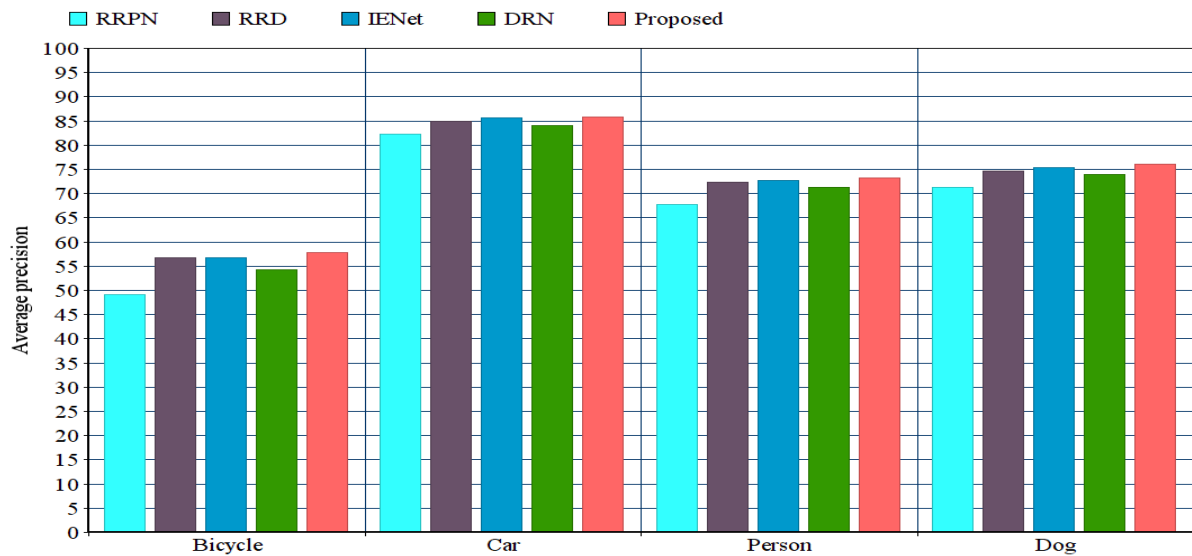
Fig. 6 Average precision for object detection

Fig. 7 demonstrates the average loss in several categories into the training set as the consistent weight values. The data is available in the training set and it is computed from the basic weight related data, the background class is not calculated in the average loss. The proposed technique has to compute the values of weight without considering the background of the remaining classes. The weight of every class is computed through the loss value and the performance of every category with the truth values have to be computed for maintaining the balance within the object classes and background values.
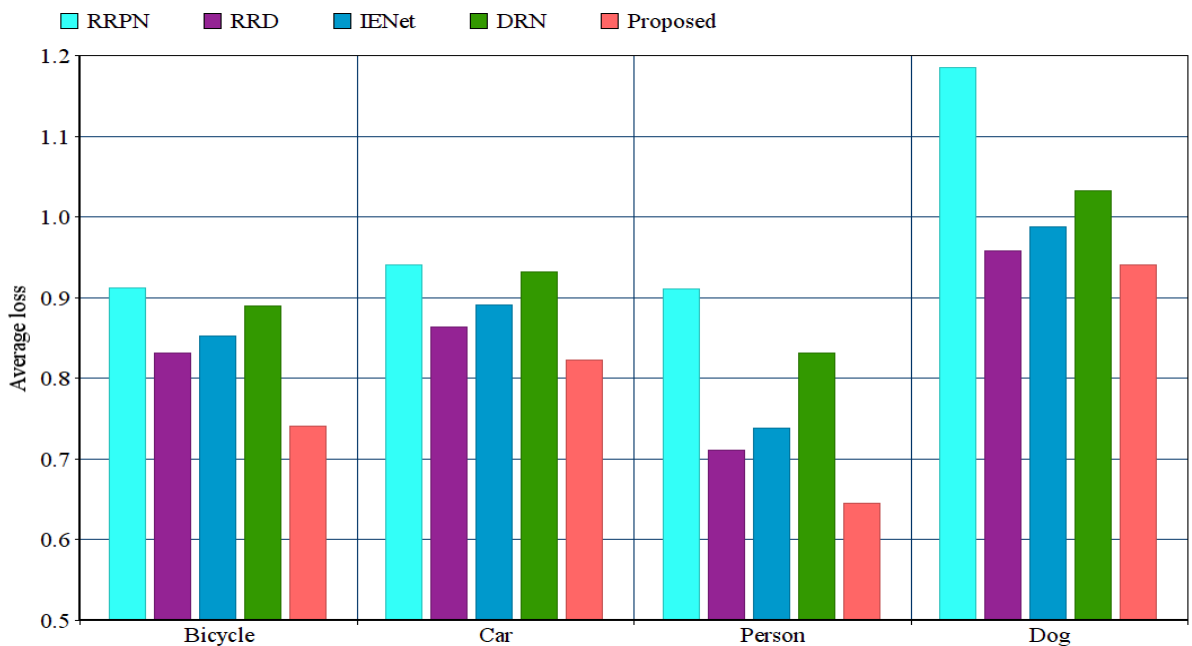

Fig. 7 Average loss for object detection

Some images are used for visualization and the object detection result is demonstrated in Fig. 8 that the results are better from left to right and the proposed framework with the Bet gradient value is more accurate than the relevant techniques as the tiny objects in far distance has been detected and several images which are not labeled from ground truth are detected well, this proves the accuracy of the proposed model.

RRPN   RRD   IENet

DRN   Proposed

Fig. 8 Object detection results

6. Conclusion

The class imbalance into the background part is identified than the remaining parts in the input images that have been enhanced the performance of the proposed hybrid deep learning algorithm in this paper. The mAP performance metric is used to design the strategy for indicating and solving the imbalance problem more effectively. The diversity data is used for enhanced sampling with identifying the uncertainty data for framing the proposed technique. The Loss related weight algorithm is implemented for adapting and providing the solution to the aggregation related problems. The class imbalance has been eliminated with the Bet gradient and Batch gradient values; the mean loss value is utilized as the impact for increasing the mAP. A sampling process is constructed for selecting the samples in spite of diversity and also the uncertainty.

7. Conflicts of Interest

The authors declare no conflict of interest.

Reference

[1]. Ashwani Kumar, Zuopeng Justin Zhang & Hongbo Lyu, Object detection in real time based on improved single shot multi-box detector algorithm, EURASIP Journal on Wireless Communications and Networking, vol. 2020, 204, 2020.
[2]. J. Redmon, S.Divvala, R.Girshick, A. Farhadi, You only look once: Unified, real-time object detection. In Proceedings of the IEEE conference on computer vision and pattern recognition (pp. 779-788) (2016).
[3]. V. Thakar, W. Ahmed, M.M.Soltani, J.Y. Yu, Ensemble-based adaptive single-shot multi-box detector. In 2018 International Symposium on Networks, Computers and Communications (ISNCC) (pp. 1-6) (2018, June). IEEE.
[4]. J.Q. Wang,J.S. Li,X.W. Zhou,X. Zhang, Improved SSD algorithm and its performance analysis of small target detection in remote sensing images[J]. Acta Optica Sinica, 39(6): 0628005(2019).
[5]. T.Y. Lin, P. Goyal, R.Girshick, K. He, P. Dollár, Focal loss for dense object detection. In Proceedings of the IEEE international conference on computer vision (pp. 2980-2988) (2017).
[6]. Nhat-Duy Nguyen, Tien Do, Thanh Duc Ngo, Duy-Dinh Le, An Evaluation of Deep Learning Methods for Small Object Detection, Journal of Electrical and Computer Engineering, vol. 2020, 3189691, pp. 1-18, 2020.
[7]. Y. Zhang et al., "Detecting Object Open Angle and Direction Using Machine Learning," in IEEE Access, vol. 8, pp. 12300-12306, 2020.
[8]. Y.J. Cao, G.M. Xu, G.C. Shi, Low altitude armored target detection based on rotation invariant faster R-CNN[J]. Laser & Optoelectronics Progress, 55(10): 101501(2018).
[9]. Liming Zhou, Chang Zheng, Haoxin Yan, Xianyu Zuo, Baojun Qiao, Bing Zhou, Minghu Fan, Yang Liu, Vehicle Detection in Remote Sensing Image Based on Machine Vision, Computational Intelligence and Neuroscience, vol. 2021, Article ID 8683226, pp. 1-12, 2021.
[10]. J. Jeong, H. Park, N. Kwak, Enhancement of SSD by concatenating feature maps for object detection. arXiv preprint arXiv:1705.09587. (2017).
[11]. J.Q. Wang,J.S. Li,X.W. Zhou,X. Zhang, Improved SSD algorithm and its performance analysis of small target detection in remote sensing images[J]. Acta Optica Sinica, 39(6): 0628005(2019).
[12]. Wang., Ding, YD. A Novel Fine-Grained Method for Vehicle Type Recognition Based on the Locally Enhanced PCANet Neural Network. J. Comput. Sci. Technol. 33, 335–350 (2018).
[13]. Jiang, R. Luo, J. Mao, T. Xiao, Y. Jiang, Acquisition of localization confidence for accurate object detection. In Proceedings of the European Conference on Computer Vision (ECCV) (pp. 784-799) (2018).
[14]. Li Guo, Yu Liao, Daisheng Luo, Honghua Liao, Generic Object Detection Using Improved Gentleboost Classifier, Physics Procedia, vol. 25, 2012, pp. 1528-1535
[15]. Free Flir Thermal Dataset for Algorithm Training. Available online: https://www.flir.com/oem/adas/adas-dataset-form/
[16]. Ma, J.; Shao, W.; Ye, H.; Wang, L.; Wang, H.; Zheng, Y.; Xue, X. Arbitrary-oriented scene text detection via rotation proposals. IEEE Trans. Multimed. 2018, 20, 3111–3122.
[17]. Liao, M.; Zhu, Z.; Shi, B.; Xia, G.S.; Bai, X. Rotation-Sensitive Regression for Oriented Scene Text Detection. In Proceedings of the IEEE Conference on Computer Vision and Pattern Recognition (CVPR), Salt Lake City, UT, USA, 18–22 June 2018.
[18]. Lin, Y.; Feng, P.; Guan, J. Ienet: Interacting embranchment one stage anchor free detector for orientation aerial object detection. arXiv 2019, arXiv:1912.00969.
[19]. Pan, X.; Ren, Y.; Sheng, K.; Dong,W.; Yuan, H.; Guo, X.; Xu, C. Dynamic refinement network for oriented and densely packed object detection. In Proceedings of the IEEE Conference on Computer Vision and Pattern Recognition, Seattle, WA, USA, 14–19, June 2020; pp. 11207–11216.

Authors Profile

Mr. Sreehari Patibandla, Research Scholar in Department of Computer Science & Engineering, Annamalai University, Chidambaram, Tamil Nadu, India. Received B.E in 2009 & M.E in 2012 in Computer Science & Engineering from Anna University, Area of interest Image & Video Processing.

Dr. Maruthavanan Archana, presently working as Assistant Professor in Department of Information Technology, Faculty of Engineering and Technology, Received my B.E degree in Information technology & awarded Gold Medal in 2007 from Annamalai University, M.E degree in Computer Science & Engineering in 2009 from Annamalai University & Completed Ph.D in 2016 from Annamalai University, Chidambaram, Tamil Nadu, India. Areas of interest are Image & Video processing, Networks and Artificial Intelligence.

Dr Rama Chaithanya Tanguturi, presently working as Professor in Computer Science & Engineering at PACE Institute of Technology & Sciences since 2016. Received B.E degree in Electronics and Communication Engineering, Anna University in 2007. Received M.E degree in Computer Science & Engineering from Anna University in the year 2009. Completed Ph.D in 2016 from Anna University, Chennai. Areas of interest are Networks, Machine Learning, Deep Learning and Cyber Security.